

# FaceXFormer: A Unified Transformer for Facial Analysis

Kartik Narayan\* Vibashan VS\* Rama Chellappa Vishal M. Patel

{knaraya4, vvishnu2, rchella4, vpatel36}@jhu.edu

<https://kartik-3004.github.io/facexformer/>

## Abstract

*In this work, we introduce FaceXFormer, an end-to-end unified transformer model capable of performing nine facial analysis tasks including face parsing, landmark detection, head pose estimation, attribute prediction, and estimation of age, gender, race, expression, and face visibility within a single framework. Conventional methods in face analysis have often relied on task-specific designs and pre-processing techniques, which limit their scalability and integration into a unified architecture. Unlike these conventional methods, FaceXFormer leverages a transformer-based encoder-decoder architecture where each task is treated as a learnable token, enabling the seamless integration and simultaneous processing of multiple tasks within a single framework. Moreover, we propose a novel parameter-efficient decoder, FaceX, which jointly processes face and task tokens, thereby learning generalized and robust face representations across different tasks. We jointly trained FaceXFormer on nine face perception datasets and conducted experiments against specialized and multi-task models in both intra-dataset and cross-dataset evaluations across multiple benchmarks, showcasing state-of-the-art or competitive performance. Further, we performed a comprehensive analysis of different backbones for unified face task processing and evaluated our model “in-the-wild”, demonstrating its robustness and generalizability. To the best of our knowledge, this is the first work to propose a single model capable of handling nine facial analysis tasks while maintaining real-time performance at 33.21 FPS.*

## 1. Introduction

Face analysis is a crucial problem as it has broad range of application such as face verification and identification [84, 85], surveillance [22], face swapping [13], face editing [127], de-occlusion [111], 3D face reconstruction [102], retail [1], image generation [109] and face retrieval [113]. Facial analysis tasks (Figure 1 involve face

parsing [28, 98], landmarks detection [46, 125], head pose estimation [12, 124], facial attributes recognition [57, 64], age/gender/race/expression estimation [8, 43] and landmarks visibility prediction [35, 54]. Therefore, developing a generalized and robust face model for all tasks is a crucial and longstanding problem in the face community.

In recent years, significant advancements have been made in facial analysis, developing state-of-the-art methods and face libraries for various tasks [12, 13, 43, 111, 124, 125]. Despite these methods achieving promising performance, they cannot be integrated into a single pipeline due to their specialized model designs and task-specific pre-processing techniques. Furthermore, deploying multiple specialized models simultaneously is computationally intensive and impractical for real-time applications, leading to increased system complexity and resource consumption. These challenges emphasize the need for a unified model that can concurrently handle multiple facial analysis tasks efficiently (see Table 1). A single model capable of addressing multiple facial tasks is desirable because it: (1) learns a robust and generalized face representation capable of handling in-the-wild images; (2) intra-task modeling helps the models to learn task-invariant representation; and (3) simplifies deployment pipelines by reducing computational overhead and achieving real-time performance.

To this end, we introduce *FaceXFormer*, an end-to-end unified model designed for nine different facial analysis tasks, such as face parsing, landmark detection, head pose estimation, attribute recognition, age/gender/race/expression estimation and face visibility prediction. *FaceXFormer* enables task unification by leveraging the transformers and learnable tokens as its core components. Specifically, we introduce a transformer-based encoder-decoder structure, treating each facial analysis task as a unique, learnable token within the framework. Treating each task as a token allows for the simultaneous processing of multiple facial analysis tasks, overcoming the challenges present in conventional methods that depend on separate, task-specific models and pre-processing routines. Furthermore, we introduce a parameter-efficient decoder, FaceX, which processes both face and task tokens together, en-

\*Equal contribution



Figure 1. *FaceXFormer* an end-to-end unified transformer model for 9 different facial analysis tasks such as face parsing, landmark detection, head pose estimation, attributes recognition, and estimation of age, gender, race, expression and face visibility.

abling the model to learn robust face representations that generalize across various tasks. This parameter-efficient design reduces computational load and allows our model to perform in real-time. After modeling the intra-task and face-token relationships in the FaceX decoder, the task tokens are fed into a unified head, which essentially converts these task tokens into corresponding task predictions.

Our extensive experiments demonstrate that *FaceXFormer* achieves state-of-the-art or competitive performance compared to specialized models and existing multi-task frameworks, including both intra-dataset and cross-dataset evaluations across multiple benchmarks. Specifically, recent multi-task frameworks such as Faceptor [67], QFace [83], and Swinface [66] address fewer tasks than *FaceXFormer*, yet our model outperforms them on existing benchmarks. Moreover, we show that our model effectively handles images ‘in the wild,’ demonstrating its robustness and generalizability across nine different tasks. This robustness is critical for real-world applications where uncontrolled conditions and diverse inputs are common. Achieving real-time performance at 33.21 FPS marks a significant advancement, making *FaceXFormer* highly suitable for time-sensitive applications. To the best of our knowledge, this is the first work to propose a single model capable of handling nine different facial analysis tasks using transformers, all while maintaining real-time performance.

In summary, our paper’s contributions are as follows:

1. We introduce *FaceXFormer*, a unified transformer-based framework capable of simultaneously processing nine different facial analysis tasks, achieving real-time performance of 33.21 FPS.
2. We propose *FaceX*, a parameter-efficient decoder that represents each facial analysis task as a token, enabling joint processing of face and task tokens.
3. We conduct extensive experiments and analyses, including both intra-dataset and cross-dataset evaluations, demonstrating that our approach achieves state-of-the-art performance when compared to existing specialized and multi-task models across multiple tasks.

## 2. Related Work

**Facial analysis tasks:** Facial analysis tasks involve face parsing [11, 28, 62, 86, 98, 122], landmarks detection [37, 41, 46, 55, 125], head pose estimation [12, 90, 115, 124], facial attributes recognition [57, 64, 80, 123], age/gender/race estimation [8, 36, 39, 43] and landmarks visibility prediction [35, 54]. These tasks hold significance in various applications such as face swapping [13, 60], face editing [127], de-occlusion [111], 3D face reconstruction [102], driver assistance [59], human-robot interaction [81], retail [1], face verification and identification [84, 85], image generation [109], image retrieval [113] and surveillance [22, 61]. Specialized models excel in their respective tasks but cannot be easily integrated with other tasks due to the need for

| Methods                   | FP | LD | HPE | Attr | Age | Gen | Race | Vis | Exp |
|---------------------------|----|----|-----|------|-----|-----|------|-----|-----|
| <b>Single-Task Models</b> |    |    |     |      |     |     |      |     |     |
| EAGR [86]                 | ✓  |    |     |      |     |     |      |     |     |
| AGRNET [87]               | ✓  |    |     |      |     |     |      |     |     |
| DML-CSR [122]             | ✓  |    |     |      |     |     |      |     |     |
| FP-LIIF [76]              | ✓  |    |     |      |     |     |      |     |     |
| Wing [20]                 |    | ✓  |     |      |     |     |      |     |     |
| HIH [37]                  |    | ✓  |     |      |     |     |      |     |     |
| DeCaFa [14]               |    | ✓  |     |      |     |     |      |     |     |
| HRNet [92]                |    | ✓  |     |      |     |     |      |     |     |
| SLPT [106]                |    | ✓  |     |      |     |     |      |     |     |
| FDN [117]                 |    |    | ✓   |      |     |     |      |     |     |
| WHENet [124]              |    |    | ✓   |      |     |     |      |     |     |
| TriNet [9]                |    |    | ✓   |      |     |     |      |     |     |
| img2pose [3]              |    |    | ✓   |      |     |     |      |     |     |
| TokenHPE [115]            |    |    | ✓   |      |     |     |      |     |     |
| SSPL [80]                 |    |    |     | ✓    |     |     |      |     |     |
| VOLO-D1 [36]              |    |    |     |      | ✓   |     |      |     |     |
| DLDL-v2 [21]              |    |    |     |      | ✓   |     |      |     |     |
| 3DDE [89]                 |    |    |     |      |     |     |      | ✓   |     |
| MNN [90]                  |    |    |     |      |     |     |      | ✓   |     |
| KTN [40]                  |    |    |     |      |     |     |      |     | ✓   |
| DMUE [77]                 |    |    |     |      |     |     |      |     | ✓   |
| <b>Multi-Task Models</b>  |    |    |     |      |     |     |      |     |     |
| SSP+SSG [30]              | ✓  |    |     | ✓    |     |     |      |     |     |
| Hetero-FAE [24]           |    |    |     | ✓    | ✓   | ✓   | ✓    |     | ✓   |
| FairFace [31]             |    |    |     |      | ✓   | ✓   | ✓    |     |     |
| MiVOLO [36]               |    |    |     |      | ✓   | ✓   |      |     |     |
| MTL-CNN [131]             |    | ✓  |     | ✓    |     |     |      |     | ✓   |
| ProS [15]                 | ✓  | ✓  |     | ✓    |     |     |      |     |     |
| FaRL [123]                | ✓  | ✓  |     | ✓    | ✓   | ✓   |      |     |     |
| HyperFace [70]            |    | ✓  | ✓   |      |     | ✓   |      | ✓   | ✓   |
| AllinOne [71]             |    | ✓  | ✓   |      | ✓   | ✓   |      | ✓   | ✓   |
| Swinface [66]             |    | ✓  |     | ✓    | ✓   |     | ✓    |     | ✓   |
| QFace [83]                |    | ✓  |     | ✓    | ✓   | ✓   | ✓    |     | ✓   |
| Faceptor [67]             | ✓  | ✓  |     | ✓    | ✓   | ✓   | ✓    |     | ✓   |
| <b>FaceXFormer</b>        | ✓  | ✓  | ✓   | ✓    | ✓   | ✓   | ✓    | ✓   | ✓   |

Table 1. Comparison with representative methods under different task settings. Our proposed *FaceXFormer* can perform various facial analysis tasks in a single model. FP - Face Parsing, LD - Landmarks Detection, HPE - Head Pose Estimation, Attr - Attributes Recognition, Age - Age, Gen - Gender, Race - Race Estimation, Exp - Facial Expression Recognition, and Vis - Face Visibility

extensive task-specific pre-processing [47, 125]. Generally, these models under-perform when applied to tasks beyond their specialization as their design is specific to their designated tasks. Some works [26, 56, 119, 121] perform multiple tasks simultaneously but utilize the additional tasks for guidance or auxiliary loss calculation to enhance the performance of the primary task. HyperFace [70] and AllinOne [71] are early models that explore multi-task learning with the aim of performing multiple tasks. HyperFace utilizes multi-scale features from different layers of CNNs, and is capable of landmarks detection, head pose estimation and gender estimation, while AllinOne additionally performs face recognition and age estimation. Recent models, such as SwinFace [66], QFace [83], and Faceptor [67], leverage transformer models with learnable tokens to perform multi-task learning. However, they perform fewer tasks, neglecting more complex ones such as

head pose estimation, landmark estimation, and face parsing. The proposed *FaceXFormer* addresses all these tasks, alongside others, and achieves state-of-the-art performance in majority of them.

**Unified transformer models:** In recent years, the rise of transformers [17, 91] have paved the way for the unification of multiple tasks within a single architecture. Unified transformer architectures are being explored across various computer vision problems, including segmentation [44, 132], visual question answering (VQA) [93, 112], tracking [96, 126], detection [97]. While these models may not achieve state-of-the-art (SOTA) performance and may under-perform compared to specialized models on some tasks, they demonstrate competitive performance across a variety of tasks. Such unification efforts have led to the development of foundational models like SAM [34], CLIP [68], LLaMA [88], GPT-3 [6], DALL-E [69], etc. However, these models are computationally intensive and not suitable for facial analysis applications that require real-time performance. Motivated by this challenge, we propose *FaceXFormer*: the first lightweight, transformer-based model capable of performing multiple facial analysis tasks. It delivers real-time performance at 33.21 FPS and can be seamlessly integrated into existing systems providing additional annotations for the person of interest.

### 3. FaceXFormer

In our framework, we follow a standard encoder-decoder structure as illustrated in Fig. 2. For an input face image  $\mathbf{I} \in \mathbb{R}^{H \times W \times 3}$ , we extract coarse to fine-grained multi-scale features  $\mathbf{S}_i$ , where  $i$  belongs to the  $i$ -th encoder output. To learn a unified face representation  $\mathbf{F}$ , these multi-scale features are then fused using a lightweight MLP-Fusion  $\mathbf{M}$  module. Following fusion, we initialize a series of task-specific tokens  $\mathbf{T} = \langle T_1, \dots, T_n \rangle$ , with each  $t_i$  representing a face task. Afterward, we initialize task tokens  $\mathbf{T} = \langle T_1, \dots, T_n \rangle$ , where  $T_i$  denotes each task. Face tokens  $\mathbf{F}$  and task tokens  $\mathbf{T}$  are then processed by a Parameter-efficient Decoder  $\mathbf{FXDec}$  where task tokens are attended with face tokens to learn relevant task representation.

$$\langle \hat{\mathbf{T}} \rangle = \mathbf{FXDec}(\langle \mathbf{F}, \mathbf{T} \rangle; \mathbf{S}_i)$$

Here,  $\hat{\mathbf{T}}$  represents the output task tokens. These tokens are then fed into unified heads, where each task token is refined and passed to its respective task head for prediction.

#### 3.1. Multi-scale Encoder

In the encoder, we employ a multi-scale encoding strategy to address the varying feature requirements intrinsic to each face analysis task. For instance, age estimation requires a global representation, while face parsing necessitates a fine-grained representation. Given an input image  $\mathbf{I}$ , it is

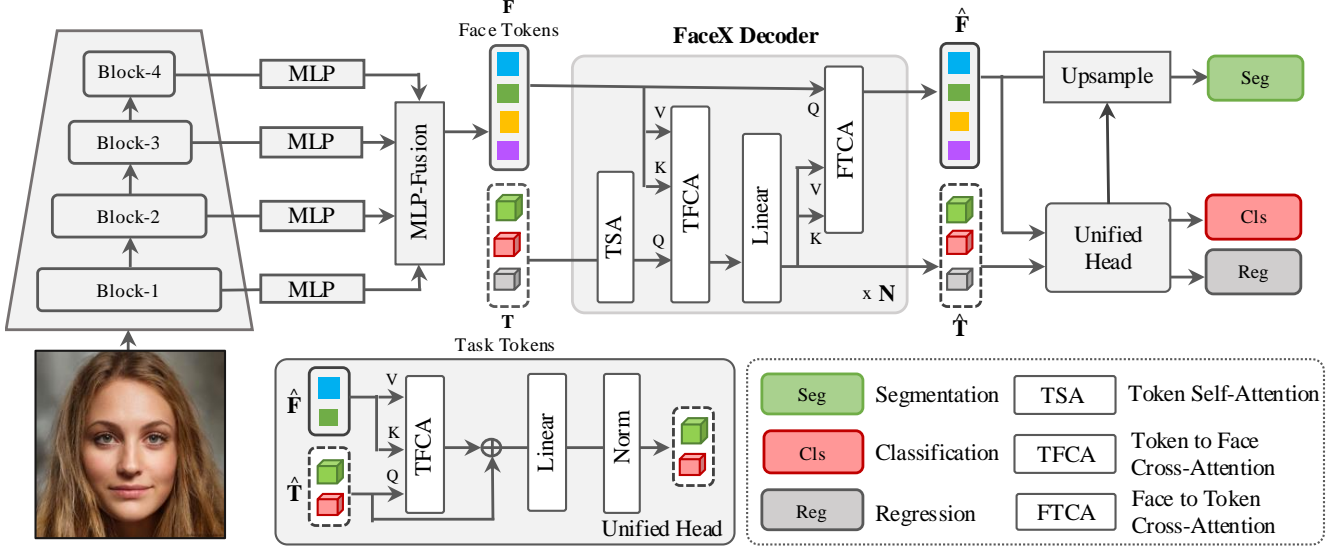


Figure 2. Overview of our proposed framework. The *FaceXFormer* employs an encoder-decoder architecture, extracting multi-scale features from the input face image  $I$ , and fusing them into a unified representation  $F$  via MLP-Fusion. Task tokens  $T$  are processed alongside face representation  $F$  in the FaceX Decoder **FXDec**, resulting in refined task-specific tokens  $\hat{T}$ . These refined tokens are then used for task-specific predictions by passing through the unified head.

processed through a set of encoder layers. For each encoder layer, the output captures information at varying levels of abstraction and detail, generating multi-scale features  $\{S_i\}_{i=1}^n$ , where  $i$  ranges from 1 to 4. This results in a hierarchical structure of features, wherein each feature map  $S_i$  transitions from a coarse to a fine-grained representation suitable for diverse facial analysis tasks.

**Lightweight MLP-Fusion:** Assigning each feature-map  $S_i$  to each face task is sub-optimal; rather, learning a unified face representation is more optimal and parameter-efficient. Following [107], we utilize a Lightweight MLP-Fusion module  $M$  to generate a fused face representation from the multi-scale features  $\{S_i\}_{i=1}^n$ . In this framework, each feature map  $S_i$  is initially passed through a separate MLP layer, standardizing the channel dimensions across scales to facilitate fusion. The transformed features are then concatenated and passed through a fusion MLP layer to aggregate a fused representation  $F$  as follows:

$$\begin{aligned}\hat{S}_i &= \text{MLP}_{\text{proj}}(D_i, D_t)(S_i), \forall i \in \{1, \dots, n\}, \\ F_{\text{cat}} &= \text{Concat}(\hat{S}_1, \hat{S}_2, \dots, \hat{S}_n), \\ F &= \text{MLP}_{\text{fusion}}(nD_t, D_t)(F_{\text{cat}}),\end{aligned}$$

where  $D_i$  and  $D_t$  are the multi-scale feature channel dimensions of  $S_i$  and the target channel dimension, respectively. The lightweight MLP-fusion design ensures minimal computational overhead while maintaining the ability to perform efficient feature fusion, which is crucial for real-time application based face analysis tasks.

### 3.2. FaceX Decoder

Detection transformer (DETR) [10] employs object tokens to learn bounding box predictions for each object. Inspired by this approach, we introduce Task Tokens, whereby each task token is designed to learn specific facial tasks leveraging the fused face representation. However, existing decoders such as DETR [10] and Deformable-DETR [129] are computationally intensive, impacting runtime significantly. To address this, we propose a FaceX (FXDec) a parameter-efficient decoder designed to efficiently model the task tokens with face tokens. Specifically, each task token learns a task-related representation by interacting with other task tokens  $T$  and face tokens  $F$ , enhancing the overall representation. The Parameter-Efficient Decoder comprises three main components: 1) Task Self-Attention, 2) Task-to-Face Cross-Attention, and 3) Face-to-Task Cross-Attention as illustrated in Fig. 2.

**Task Self-Attention (TSA):** The Task Self-Attention module is designed to refine the task-specific representations within the set of task tokens  $T = \langle T_1, \dots, T_n \rangle$ . Each task token  $T_i$  is an embedded representation that corresponds to a specific facial task. In TSA, each  $T_i$  is updated by attending to all other task tokens to capture task-specific interactions. Formally, the updated task token  $T'_i$  is computed as:

$$T'_i = \text{SelfAttn}(Q = T'_i, K = T, V = T),$$

where Attention denotes the multi-headed self-attention mechanism, and  $Q$ ,  $K$ , and  $V$  represent the queries, keys, and values, respectively. Therefore, TSA essentially helps



the model to learn task-invariant representation.

**Task-to-Face Cross-Attention (TFCA):** The Task-to-Face Cross-Attention module allows each task token to interact with the fused face representation  $\mathbf{F}$ . This enables each task token to gather information relevant to its specific facial task from the fused face features. In this module, the fused face representation  $\mathbf{F}$  acts as both key and value, while the task tokens serve as queries. The updated task token  $\hat{T}_i$  is then computed as follows:

$$\hat{T}_i = \text{CrossAttn}(\mathbf{Q} = T'_i, \mathbf{K} = \mathbf{F}, \mathbf{V} = \mathbf{F}),$$

where  $\hat{\mathbf{T}} = \langle \hat{T}_1, \dots, \hat{T}_n \rangle$  is the output task token. Thus, TFCA enables direct interaction between the task-specific tokens and the compact facial features, facilitating task-focused feature extraction.

**Face-to-Task Cross-Attention (FTCA):** Conversely, the Face-to-Task Cross-Attention module is designed to refine the fused face representation  $\mathbf{F}$  based on the information from the updated task tokens. This process aids in enhancing the face representation with task-specific details, thereby improving the extraction of overall fused representation. In FTCA, the set of updated task tokens  $\mathbf{T}' = \{T'_1, T'_2, \dots, T'_m\}$  acts as both keys and values, while the fused face features  $\mathbf{F}$  serve as queries. The refined face representation  $\hat{\mathbf{F}}$  is computed as:

$$\hat{\mathbf{F}} = \text{CrossAttn}(\mathbf{Q} = \mathbf{F}, \mathbf{K} = \mathbf{T}', \mathbf{V} = \mathbf{T}').$$

Through this inverse attention mechanism, the face representation is augmented with critical task-specific details, enabling a robust approach towards facial task unification.

### 3.3. Unified-Head

In Unified-Head, the task tokens are processed to obtain corresponding task predictions. As shown in Fig. 2, the output face tokens  $\hat{\mathbf{F}}$  and task tokens  $\hat{\mathbf{T}}$  are processed through a Task-to-Face Cross-Attention mechanism to obtain final refined features. Then, the output tokens are fed into their corresponding task heads. The task head for landmark detection is a hourglass network and for head pose estimation is a regression MLP, while the tasks of estimating age, gender, race, expression, visibility, and attributes prediction utilize classification MLPs. For face parsing, we leverage the output  $\hat{\mathbf{F}}$  and process it through an upsampling layer, then perform a cross-product with the face parsing token to obtain a segmentation map. The number of tokens for segmentation corresponds to the total number of classes. For landmark prediction, it corresponds to the number of landmarks (i.e., 68). For head pose estimation, the number of tokens is 9, representing the  $3 \times 3$  rotation matrix. For other tasks, one token is used for each.

### 3.4. Multi-Task Training

We aim to train *FaceXFormer* for multiple facial analysis tasks simultaneously, however each task requires distinct and sometimes conflicting pre-processing steps. For instance, landmark detection typically requires keypoint alignment of faces, which contradicts the needs for head pose estimation, as it may eliminate the natural variability of headposes. Due to these reasons, integrating all tasks into a single model poses significant challenges. To address this, *FaceXFormer* incorporates task-specific tokens designed to extract task-specific features from the fused representation. These task tokens compel the backbone to learn a unified representation capable of supporting a broad spectrum of facial analysis tasks. We employ different loss functions for each task and combine them in a joint objective for training. The final loss function is given as:

$$L = \lambda_{seg} L_{seg} + \lambda_{lnd} L_{lnd} + \lambda_{hpe} L_{hpe} + \lambda_{attr} L_{attr} \\ + \lambda_a L_a + \lambda_{g/r} L_{g/r} + \lambda_{exp} L_{exp} + \lambda_{vis} L_{vis}$$

where  $L_{seg}$  is the mean of dice loss [82] and Cross-Entropy (CE) loss for face parsing,  $L_{lnd}$  is STAR loss [125] for landmarks prediction,  $L_{hpe}$  is geodesic loss [115] for head pose estimation,  $L_{g/r}$  is CE loss for gender/race estimation,  $L_a$  is mean of L1 loss and CE loss for age estimation,  $L_{exp}$  is CE loss for facial expression recognition, and  $L_{attr}$  and  $L_{vis}$  are Binary Cross-Entropy with logits loss for attributes prediction and face visibility prediction respectively.

## 4. Experiments and Results

### 4.1. Datasets and Metrics

We perform co-training, where the model is simultaneously trained for multiple tasks using a total of 9 datasets with task-specific annotations. We conduct intra-dataset and cross-dataset evaluations and present our results on the test sets according to the standard protocol for each task using the following datasets:

**Training:** *Face Parsing:* CelebAMaskHQ [38]; *Landmarks Detection:* 300W [75]; *Head Pose Estimation:* 300W-LP [128]; *Attributes Prediction:* CelebA [50]; *Facial Expression Recognition:* RAF-DB [42], AffectNet [58]; *Age/Gender/Race estimation:* UTKFace [120], FairFace [32]; *Visibility Prediction:* COFW [7].

**Test (Intra-dataset):** *Face Parsing:* CelebAMaskHQ [38]; *Landmarks Detection:* 300W [128]; *Attributes Prediction:* CelebA [50]; *Facial Expression Recognition:* RAF-DB [42]; *Age/Gender/Race Estimation:* UTKFace [120], FairFace [32]; *Visibility Prediction:* COFW [7].

**Test (Cross-dataset):** *Landmarks Detection:* 300VW [78]; *Head Pose Estimation:* BIWI [18]; *Attributes Prediction:* LFWA [101].

The evaluation metrics used are the F1-score for face parsing, Normalized Mean Error (NME) for landmark predic-

| Method                        | Input Res. | Skin        | Hair        | Nose        | L-Eye       | R-Eye       | L-Brow      | R-Brow      | L-Lip       | I-Mouth     | U-Lip       | Mean F1      |
|-------------------------------|------------|-------------|-------------|-------------|-------------|-------------|-------------|-------------|-------------|-------------|-------------|--------------|
| Wei et al. [99]               | 512        | 96.4        | 91.1        | 91.9        | 87.1        | 85.0        | 80.8        | 82.5        | 91.0        | 90.6        | 87.9        | 88.43        |
| EHANet [51]                   | 512        | 96.0        | 93.9        | 93.7        | 86.2        | 86.5        | 83.2        | 83.1        | 90.3        | <u>93.8</u> | 88.6        | 89.53        |
| EAGRNet [86]                  | 473        | 96.2        | 94.9        | <b>94.0</b> | 88.6        | 89.0        | 85.7        | 85.2        | <b>91.2</b> | <b>95.0</b> | 88.9        | 90.87        |
| AGRNet [87]                   | 473        | <u>96.5</u> | 87.6        | 93.9        | 88.7        | 89.1        | 85.5        | 85.6        | 91.1        | 92.0        | 89.1        | 89.91        |
| FaRL <sub>scratch</sub> [123] | 512        | 96.2        | 94.9        | 93.8        | 89.0        | 89.0        | 85.3        | 85.4        | 90.0        | 91.7        | 88.1        | 90.34        |
| DML-CSR [122]                 | 473        | 95.7        | 94.5        | <u>93.9</u> | <u>89.4</u> | <u>89.6</u> | 85.5        | 85.7        | <u>91.0</u> | 91.8        | <u>89.1</u> | 90.62        |
| FP-LIIF [76]                  | 256        | 96.4        | 95.1        | 93.7        | 88.5        | 88.5        | 84.5        | 84.3        | 90.3        | 92.1        | 87.5        | 90.09        |
| SwinFace [66]                 | ×          | ×           | ×           | ×           | ×           | ×           | ×           | ×           | ×           | ×           | ×           | ×            |
| QFace [83]                    | ×          | ×           | ×           | ×           | ×           | ×           | ×           | ×           | ×           | ×           | ×           | ×            |
| Faceptor [67]                 | 512        | <b>96.6</b> | <b>96.2</b> | 93.9        | 89.4        | 89.1        | <b>86.2</b> | <b>86.3</b> | 90.6        | 91.6        | 89.0        | <u>90.89</u> |
| <i>FaceXFormer</i>            | 224        | 96.4        | <u>95.7</u> | 93.8        | <b>90.1</b> | <b>90.3</b> | <u>86.0</u> | <u>85.9</u> | 90.6        | 92.1        | <b>89.2</b> | <b>92.01</b> |

Table 2. Performance comparison for face parsing on the CelebAMask-HQ dataset [38]. The symbol × indicates that the model does not perform the corresponding task. **Red** = First Best, Blue = Second Best.

tion, Mean Absolute Error (MAE) for head pose estimation and age estimation, accuracy for facial expression recognition, attributes prediction, gender estimation, race estimation, and recall at 80% precision for visibility prediction.

| Methods            | Expression (RAF-DB) | Methods            | Visibility (COFW) | Methods                | Age (MAE) UTKFace |
|--------------------|---------------------|--------------------|-------------------|------------------------|-------------------|
| DLP-CNN [42]       | 80.89               | RCPR [7]           | 40                | OR-CNN [63]            | 5.74              |
| gACNN [45]         | 85.07               | Wu et al. [105]    | 44.43             | Axel Berg et al. [4]   | 4.55              |
| IPA2LT [114]       | 86.77               | Wu et al. [104]    | 49.11             | CORAL [8]              | 5.47              |
| RAN [95]           | 86.90               | ECT [116]          | 63.4              | Gustafsson et al. [23] | 4.65              |
| CovPool [2]        | 87.00               | 3DDE [89]          | 63.89             | R50-SORD [65]          | 4.36              |
| SCN [94]           | 87.03               | MNN [90]           | <u>72.12</u>      | VOLO-D1 [36]           | 4.23              |
| DACL [19]          | 87.78               |                    |                   | DLDL-v2 [21]           | 4.42              |
| KTN [40]           | 88.07               |                    |                   | MWR [79]               | 4.37              |
| DMUE [77]          | <u>88.76</u>        |                    |                   |                        |                   |
| SwinFace [66]      | 86.54               | SwinFace [66]      | ×                 | SwinFace [66]          | ×                 |
| QFace [83]         | <b>92.86</b>        | QFace [83]         | ×                 | QFace [83]             | ×                 |
| Faceptor [67]      | 87.58               | Faceptor [67]      | ×                 | Faceptor [67]          | <b>4.10</b>       |
| <i>FaceXFormer</i> | <b>88.24</b>        | <i>FaceXFormer</i> | <b>72.56</b>      | <i>FaceXFormer</i>     | <u>4.17</u>       |

Table 3. Performance comparison on facial expression recognition, face visibility prediction and age estimation. × indicates a model that doesn’t perform the task.

## 4.2. Implementation Details

We train our models using a distributed PyTorch setup on eight A6000 GPUs, each equipped with 48GB of memory. The models’ backbones are initialized with ImageNet pre-trained weights and processes input images at a resolution of  $224 \times 224$ . We employ the AdamW optimizer with a weight decay of  $1e^{-5}$ . All models are trained for 12 epochs with a batch size of 48 on each GPU, and an initial learning rate of  $1e^{-4}$ , which decays by a factor of 10 at the  $6^{th}$  and  $10^{th}$  epochs. We train the model for three additional epochs for some tasks. For data augmentation, we randomly apply Gaussian blur, grayscale conversion, gamma correction, occlusion, horizontal flipping, and affine transformations, such as rotation, translation and scaling. The number of FaceX decoder  $N$  is set to two. To ensure stable training across tasks when using multiple datasets of varying sample sizes, we equalize the representation of each task’s samples in every batch through upsampling. Additional details on

our implementation are provided in the supplementary.

## 4.3. Main results

In Tab. 2, Tab. 4, Tab. 3, we present a comparative analysis of *FaceXFormer* with recent methods across a variety of tasks. A significant highlight of our work is its unique capability to deliver promising results across multiple tasks using a single unified model. Specifically, *FaceXFormer* achieves state-of-the-art performance in face parsing, with a mean F1 score of 92.01 on CelebAMaskHQ at a resolution of  $224 \times 224$ , which is half the input size required by other state-of-the-art methods. Furthermore, it demonstrates superior performance in head pose estimation and landmark detection, achieving a mean MAE of 3.52 and a mean NME of 4.67, respectively. Additionally, *FaceXFormer* provides a significant performance boost in attributes prediction and visibility prediction, achieving an accuracy of 91.83% on the CelebA dataset and 72.56% on COFW. It also performs competitively in age estimation, achieving the second-best score of 4.17, and achieves an accuracy of 88.24% in facial expression recognition. The results on gender estimation across different race categories is shown in Tab. 6. We present the additional cross-dataset results in Appendix B.

Recent models such as SwinFace [66], QFace [83], and Faceptor [67] also aim to unify tasks but only address a subset of them. These models tend to exclude complex tasks such as segmentation, head pose estimation, and landmark prediction due to their conflicting training objectives. In contrast, *FaceXFormer*, with its learnable task-specific tokens, seamlessly unifies these tasks and achieves state-of-the-art performance across them. It outperforms previous multi-task models in tasks such as segmentation, head pose estimation, landmark prediction, attributes prediction, and visibility prediction, while achieving the second-best performance in age estimation. In this work, we simultaneously train for nine heterogeneous tasks, presenting a more formidable challenge than previous approaches. This difficulty arises primarily from the distinct and diverse na-

| Methods            | Headpose (BIWI) |             |             |             | Methods            | Landmarks (300W) |             |             | Methods            | CelebA Acc.  |
|--------------------|-----------------|-------------|-------------|-------------|--------------------|------------------|-------------|-------------|--------------------|--------------|
|                    | Yaw             | Pitch       | Roll        | MAE         |                    | Full             | Com         | Chal        |                    |              |
| HopeNet [74]       | 4.81            | 6.61        | 3.27        | 4.89        | LAB [103]          | 3.49             | 2.98        | 5.19        | PANDA-1 [118]      | 85.43        |
| QuatNet [27]       | 5.49            | 4.01        | 2.94        | 4.15        | Wing [20]          | 4.04             | 3.27        | 7.18        | LNets+ANet [49]    | 87.33        |
| FSA-Net [110]      | 4.27            | 5.49        | 2.93        | 4.14        | DeCaFa [14]        | 3.39             | 2.93        | 5.26        | SSP+SSG [30]       | 88.24        |
| EVA-GCN [108]      | 6.01            | 4.78        | 2.98        | 3.98        | HRNet [92]         | 3.32             | 2.87        | 5.15        | MOON [73]          | 90.94        |
| TriNet [9]         | 4.11            | 4.75        | 3.04        | 3.97        | PicassoNet [100]   | 3.58             | 3.03        | 5.81        | NSA [52]           | 90.61        |
| img2pose [3]       | 4.56            | <b>3.54</b> | 3.24        | 3.78        | AVS+SAN [16]       | 3.86             | 3.21        | 6.46        | MCNN-AUX [25]      | 91.29        |
| MNN [90]           | 3.98            | 4.61        | <b>2.39</b> | 3.66        | LUVLi [35]         | 3.23             | 2.76        | 5.16        | MCFA [131]         | 91.23        |
| MFDNet [48]        | <b>3.40</b>     | 4.68        | 2.77        | <u>3.62</u> | HIH [37]           | <u>3.09</u>      | <b>2.65</b> | 4.89        | DMM-CNN [53]       | 91.70        |
| TokenHPE [115]     | 3.95            | 4.51        | 2.71        | 3.72        | PIPNet [29]        | 3.19             | 2.78        | 4.89        | SSPL [80]          | <u>91.77</u> |
| WHENet [124]       | 3.99            | 4.39        | 3.06        | 3.81        | SLPT [106]         | 3.17             | 2.75        | 4.90        | FaRL [123]         | 91.39        |
| SwinFace [66]      | ×               | ×           | ×           | ×           | SwinFace [66]      | ×                | ×           | ×           | SwinFace [66]      | 91.38        |
| QFace [83]         | –               | –           | –           | –           | QFace [83]         | ×                | ×           | ×           | QFace [83]         | 91.56        |
| Faceptor [67]      | ×               | ×           | ×           | ×           | Faceptor [67]      | 3.16             | 2.75        | <u>4.84</u> | Faceptor [67]      | 91.39        |
| <b>FaceXFormer</b> | <u>3.91</u>     | <u>3.97</u> | <u>2.67</u> | <b>3.52</b> | <b>FaceXFormer</b> | <b>3.05</b>      | <u>2.66</u> | <b>4.67</b> | <b>FaceXFormer</b> | <b>91.83</b> |

Table 4. Performance comparison on headpose, landmark detection, and attribute recognition. The symbol × indicates that the model does not perform the corresponding task, while – denotes that results for this dataset are not provided. **Red** = First Best, Blue = Second Best.

| Backbone   | Seg   | Reg  | Cls   | FPS   | Params |
|------------|-------|------|-------|-------|--------|
| MobileNet  | 91.21 | 4.64 | 88.22 | 39.76 | 25.32  |
| ResNet101  | 91.49 | 4.37 | 88.91 | 34.98 | 65.54  |
| ConvNext-B | 92.08 | 4.35 | 89.09 | 36.61 | 110.19 |
| Swin-B     | 92.01 | 4.12 | 90.03 | 33.21 | 109.29 |

Table 5. Effect of different backbones on performance and FPS.

ture of the tasks, which require task-specific features, pre-processing steps, and often conflicting training objectives. Despite these challenges, *FaceXFormer* effectively handles multiple tasks, delivering SOTA or competitive performance, thereby establishing itself as a unified SOTA model.

#### 4.4. Qualitative “in-the-wild” results

In this section, we present the qualitative results of *FaceXFormer* on randomly selected “in-the-wild” images. We select three random images and showcase the results for face parsing, head pose estimation, landmarks prediction, age estimation, gender and race classification, and attributes prediction in Figure 3. Notably, the model successfully performs complex tasks such as face segmentation, head pose estimation, and landmark prediction, even when the input samples are out-of-distribution. Furthermore, *FaceXFormer* can be effectively used as a tool to generate multiple annotations for each image, making it valuable for various downstream tasks. These results highlight *FaceXFormer’s* robust performance in challenging, real-world scenarios.

### 5. Ablation Study

In this section, we explore the impact of various backbones and their sizes on performance. Additionally, we highlight

that the proposed model exhibits minimal bias compared to other models by performing age and gender prediction across different various. We provide additional ablation of different components in our model in the supplementary.

#### 5.1. Effect of different backbone and different size.

In Table 5, we present experiments analyzing the impact of different backbones and their sizes on *FaceXFormer*. We group head pose estimation, landmarks prediction, and age estimation into the regression (Reg) category, while attributes prediction and facial expression recognition are categorized as classification (Cls). ConvNeXt achieves the best performance in segmentation with an F1 score of 92.08%. The Swin Transformer backbone excels in both regression and classification tasks, with a mean error of 4.12 and a mean accuracy of 90.03%, respectively. In contrast, MobileNet demonstrates the lowest performance metrics, including an F1 score of 91.21% and a mean error of 4.64, highlighting its limitations in handling larger, more complex datasets due to its smaller receptive field compared to the Swin Transformer. The selection of the Swin Transformer as the backbone for *FaceXFormer* is driven by its superior scalability and global contextual understanding, both of which are essential for facial analysis tasks. Furthermore, *FaceXFormer* achieves real-time performance at 33.21 FPS.

#### 5.2. Bias Analysis and Ethical Considerations

In our work, we utilize a total of 12 datasets for training and evaluation. We obtained these datasets following the procedures stated on their respective pages and signed the license agreements if and when necessary. As we train our models on multiple datasets designed for different tasks, the

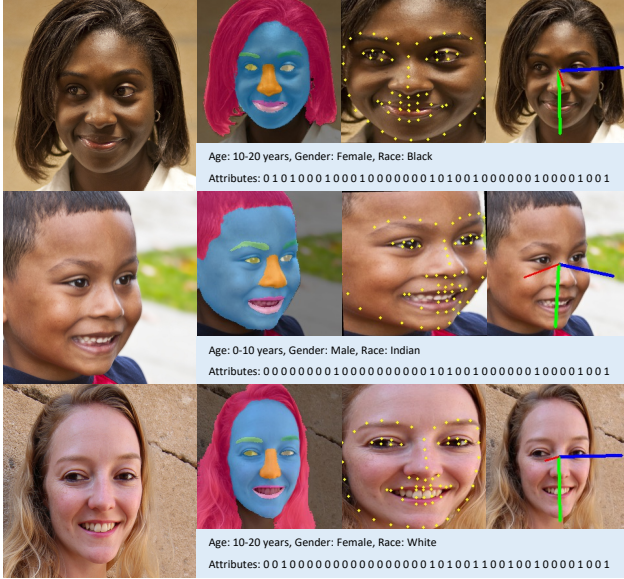


Figure 3. *FaceXFormer* predictions on “in-the-wild” images

|        | Model       | Data Points | White | Non-white | Average | Discrepancy |
|--------|-------------|-------------|-------|-----------|---------|-------------|
| Age    | FairFace    | 100K        | 60.05 | 60.63     | 60.52   | 0.58        |
|        | CLIP        | 400M        | 62.25 | 61.95     | 62.00   | -0.30       |
|        | FaRL        | 20M         | 61.49 | 61.84     | 61.78   | 0.35        |
|        | FaceXFormer | 400K        | 58.94 | 59.44     | 59.34   | 0.50        |
| Gender | FairFace    | 100K        | 94.15 | 94.41     | 94.36   | 0.26        |
|        | CLIP        | 400M        | 94.87 | 95.78     | 95.61   | 0.91        |
|        | FaRL        | 20M         | 95.16 | 95.77     | 95.65   | 0.61        |
|        | FaceXFormer | 400K        | 95.34 | 95.19     | 95.22   | -0.09       |

Table 6. Age and gender accuracy w.r.t race groups on FairFace

subjects across different age groups, genders, and races is not equal. This imbalance may introduce bias in the model. Therefore, we provide an analysis using the FairFace [31] dataset, which is balanced in terms of age, gender and race. We follow [68] and define the “Non-white” group to include multiple racial categories: “Black”, “Indian”, “East Asian”, “Southeast Asian”, “Middle Eastern” and “Latino”. As can be seen from Table 6, *FaceXFormer* shows the smallest performance discrepancy across different racial groups and exhibits minimal bias compared to other models despite being trained on fewer data points. This can be attributed to race estimation being the task in co-training.

## 6. Discussions

**Broader Impact:** The world is moving towards transformers because of its potential to model large amounts of data [5, 6, 34]. Presently, the face community lacks large-scale annotated datasets to train foundational models capable of performing a wide spectrum of facial tasks. The largest clean dataset, WebFace42M [130], lacks annotations for face parsing, landmarks detection and attributes recognition. *FaceXFormer* can be used as an annotator for large-

scale data, and can be continually improved through successive rounds of annotation and fine-tuning. We aim to propel the face community towards developing foundation models that cater to a variety of facial tasks. Additionally, *FaceXFormer* is a lightweight model that provides real-time output based on task-specific queries and can be appended with existing facial systems to provide additional information. It can also serve as a valuable tool in surveillance, and provide auxiliary information for subject analysis and image retrieval.

**Limitations:** We recognize certain limitations of the proposed *FaceXFormer*, particularly the requirement for complete retraining to add a new task, which may reduce its flexibility. Furthermore, although it includes token support for multiple tasks, it lacks interactivity and full promptability. Nonetheless, *FaceXFormer* is distinct in its ability to handle up to 9 heterogeneous tasks within a single model, achieving state-of-the-art or competitive performance across these tasks in real-time, making it well-suited for deployment. Future work will focus on developing a large-scale pre-trained foundational model with zero-shot capabilities.

## 7. Conclusion

In conclusion, the *FaceXformer* introduces a novel end-to-end unified model that efficiently handles a comprehensive range of facial analysis tasks in real-time. By adopting a transformer-based encoder-decoder architecture and treating each task as a learnable token, our approach successfully integrates multiple tasks within a single framework. The proposed parameter-efficient decoder, FaceX, enhances the model’s ability to learn robust and generalized face representations across diverse tasks. Our comprehensive experiments demonstrate that the proposed model achieves state-of-the-art performance across multiple facial analysis tasks. Additionally, training on multiple datasets leads to better representation learning. In conclusion, we demonstrate that facial tasks can be treated as tokens, leading to the unification of tasks; following this, we hope our work provides a foundation for developing large models capable of performing multiple facial analysis tasks.

## 8. Acknowledgment

This research is based upon work supported in part by the Office of the Director of National Intelligence (ODNI), Intelligence Advanced Research Projects Activity (IARPA), via [2022-21102100005]. The views and conclusions contained herein are those of the authors and should not be interpreted as necessarily representing the official policies, either expressed or implied, of ODNI, IARPA, or the U.S. Government. The US Government is authorized to reproduce and distribute reprints for governmental purposes notwithstanding any copyright annotation therein.



## References

- [1] B Abirami, TS Subashini, and V Mahavaishnavi. Gender and age prediction from real time facial images using cnn. *Materials Today: Proceedings*, 33:4708–4712, 2020. 1, 2
- [2] Dinesh Acharya, Zhiwu Huang, Danda Pani Paudel, and Luc Van Gool. Covariance pooling for facial expression recognition. In *Proceedings of the IEEE conference on computer vision and pattern recognition workshops*, pages 367–374, 2018. 6
- [3] Vitor Albiero, Xingyu Chen, Xi Yin, Guan Pang, and Tal Hassner. img2pose: Face alignment and detection via 6dof, face pose estimation. In *Proceedings of the IEEE/CVF conference on computer vision and pattern recognition*, pages 7617–7627, 2021. 3, 7
- [4] Axel Berg, Magnus Oskarsson, and Mark O’Connor. Deep ordinal regression with label diversity. In *2020 25th international conference on pattern recognition (ICPR)*, pages 2740–2747. IEEE, 2021. 6
- [5] Tim Brooks, Bill Peebles, Connor Holmes, Will DePue, Yufei Guo, Li Jing, David Schnurr, Joe Taylor, Troy Luhman, Eric Luhman, Clarence Ng, Ricky Wang, and Aditya Ramesh. Video generation models as world simulators, 2024. 8
- [6] Tom Brown, Benjamin Mann, Nick Ryder, Melanie Subbiah, Jared D Kaplan, Prafulla Dhariwal, Arvind Neelakantan, Pranav Shyam, Girish Sastry, Amanda Askell, et al. Language models are few-shot learners. *Advances in neural information processing systems*, 33:1877–1901, 2020. 3, 8
- [7] Xavier P Burgos-Artizzu, Pietro Perona, and Piotr Dollár. Robust face landmark estimation under occlusion. In *Proceedings of the IEEE international conference on computer vision*, pages 1513–1520, 2013. 5, 6, 17
- [8] Wenzhi Cao, Vahid Mirjalili, and Sebastian Raschka. Rank consistent ordinal regression for neural networks with application to age estimation. *Pattern Recognition Letters*, 140:325–331, 2020. 1, 2, 6
- [9] Zhiwen Cao, Zongcheng Chu, Dongfang Liu, and Yingjie Chen. A vector-based representation to enhance head pose estimation. In *Proceedings of the IEEE/CVF Winter Conference on applications of computer vision*, pages 1188–1197, 2021. 3, 7
- [10] Nicolas Carion, Francisco Massa, Gabriel Synnaeve, Nicolas Usunier, Alexander Kirillov, and Sergey Zagoruyko. End-to-end object detection with transformers. In *European conference on computer vision*, pages 213–229. Springer, 2020. 4
- [11] Liang-Chieh Chen, Yi Yang, Jiang Wang, Wei Xu, and Alan L Yuille. Attention to scale: Scale-aware semantic image segmentation. In *Proceedings of the IEEE conference on computer vision and pattern recognition*, pages 3640–3649, 2016. 2
- [12] Alejandro Cobo, Roberto Valle, José M Buenaposada, and Luis Baumela. On the representation and methodology for wide and short range head pose estimation. *Pattern Recognition*, 149:110263, 2024. 1, 2
- [13] Kaiwen Cui, Rongliang Wu, Fangneng Zhan, and Shijian Lu. Face transformer: Towards high fidelity and accurate face swapping. In *Proceedings of the IEEE/CVF Conference on Computer Vision and Pattern Recognition*, pages 668–677, 2023. 1, 2
- [14] Arnaud Dapogny, Kevin Bailly, and Matthieu Cord. De-cafa: Deep convolutional cascade for face alignment in the wild. In *Proceedings of the IEEE/CVF International Conference on Computer Vision*, pages 6893–6901, 2019. 3, 7
- [15] Xing Di, Yiyu Zheng, Xiaoming Liu, and Yu Cheng. Pros: Facial omni-representation learning via prototype-based self-distillation. In *Proceedings of the IEEE/CVF Winter Conference on Applications of Computer Vision*, pages 6087–6098, 2024. 3
- [16] Xuanyi Dong, Yan Yan, Wanli Ouyang, and Yi Yang. Style aggregated network for facial landmark detection. In *Proceedings of the IEEE conference on computer vision and pattern recognition*, pages 379–388, 2018. 7
- [17] Alexey Dosovitskiy, Lucas Beyer, Alexander Kolesnikov, Dirk Weissenborn, Xiaohua Zhai, Thomas Unterthiner, Mostafa Dehghani, Matthias Minderer, Georg Heigold, Sylvain Gelly, et al. An image is worth 16x16 words: Transformers for image recognition at scale. *arXiv preprint arXiv:2010.11929*, 2020. 3
- [18] Gabriele Fanelli, Matthias Dantone, Juergen Gall, Andrea Fossati, and Luc Van Gool. Random forests for real time 3d face analysis. *International journal of computer vision*, 101:437–458, 2013. 5, 16
- [19] Amir Hossein Farzaneh and Xiaojun Qi. Facial expression recognition in the wild via deep attentive center loss. In *Proceedings of the IEEE/CVF winter conference on applications of computer vision*, pages 2402–2411, 2021. 6
- [20] Zhen-Hua Feng, Josef Kittler, Muhammad Awais, Patrik Huber, and Xiao-Jun Wu. Wing loss for robust facial landmark localisation with convolutional neural networks. In *Proceedings of the IEEE Conference on Computer Vision and Pattern Recognition (CVPR)*, 2018. 3, 7
- [21] Bin-Bin Gao, Xin-Xin Liu, Hong-Yu Zhou, Jianxin Wu, and Xin Geng. Learning expectation of label distribution for facial age and attractiveness estimation. *arXiv preprint arXiv:2007.01771*, 2020. 3, 6
- [22] Asma El Kissi Ghalleb, Safa Boumaiza, and Najoua Es-soukri Ben Amara. Demographic face profiling based on age, gender and race. In *2020 5th International Conference on Advanced Technologies for Signal and Image Processing (ATSIP)*, pages 1–6. IEEE, 2020. 1, 2
- [23] Fredrik K Gustafsson, Martin Danelljan, Goutam Bhat, and Thomas B Schön. Energy-based models for deep probabilistic regression. In *Computer Vision—ECCV 2020: 16th European Conference, Glasgow, UK, August 23–28, 2020, Proceedings, Part XX 16*, pages 325–343. Springer, 2020. 6
- [24] Hu Han, Anil K Jain, Fang Wang, Shiguang Shan, and Xilin Chen. Heterogeneous face attribute estimation: A deep multi-task learning approach. *IEEE transactions on pattern analysis and machine intelligence*, 40(11):2597–2609, 2017. 3

- [25] Emily Hand and Rama Chellappa. Attributes for improved attributes: A multi-task network utilizing implicit and explicit relationships for facial attribute classification. In *Proceedings of the AAAI conference on artificial intelligence*, 2017. 7
- [26] Hui-Lan Hsieh, Winston Hsu, and Yan-Ying Chen. Multi-task learning for face identification and attribute estimation. In *2017 IEEE International Conference on Acoustics, Speech and Signal Processing (ICASSP)*, pages 2981–2985, 2017. 3
- [27] Heng-Wei Hsu, Tung-Yu Wu, Sheng Wan, Wing Hung Wong, and Chen-Yi Lee. Quatnet: Quaternion-based head pose estimation with multiregression loss. *IEEE Transactions on Multimedia*, 21(4):1035–1046, 2018. 7
- [28] Aaron S Jackson, Michel Valstar, and Georgios Tzimiropoulos. A cnn cascade for landmark guided semantic part segmentation. In *Computer Vision–ECCV 2016 Workshops: Amsterdam, The Netherlands, October 8–10 and 15–16, 2016, Proceedings, Part III 14*, pages 143–155. Springer, 2016. 1, 2
- [29] Haibo Jin, Shengcai Liao, and Ling Shao. Pixel-in-pixel net: Towards efficient facial landmark detection in the wild. *International Journal of Computer Vision*, 129(12):3174–3194, 2021. 7
- [30] Mahdi M Kalayeh, Boqing Gong, and Mubarak Shah. Improving facial attribute prediction using semantic segmentation. In *Proceedings of the IEEE Conference on Computer Vision and Pattern Recognition*, pages 6942–6950, 2017. 3, 7
- [31] Kimmo Karkkainen and Jungseock Joo. Fairface: Face attribute dataset for balanced race, gender, and age for bias measurement and mitigation. In *Proceedings of the IEEE/CVF winter conference on applications of computer vision*, pages 1548–1558, 2021. 3, 8
- [32] Kimmo Karkkainen and Jungseock Joo. Fairface: Face attribute dataset for balanced race, gender, and age for bias measurement and mitigation. In *Proceedings of the IEEE/CVF Winter Conference on Applications of Computer Vision*, pages 1548–1558, 2021. 5, 17
- [33] Tero Karras, Samuli Laine, and Timo Aila. A style-based generator architecture for generative adversarial networks. In *Proceedings of the IEEE/CVF conference on computer vision and pattern recognition*, pages 4401–4410, 2019. 17
- [34] Alexander Kirillov, Eric Mintun, Nikhila Ravi, Hanzi Mao, Chloe Rolland, Laura Gustafson, Tete Xiao, Spencer Whitehead, Alexander C Berg, Wan-Yen Lo, et al. Segment anything. *arXiv preprint arXiv:2304.02643*, 2023. 3, 8
- [35] Abhinav Kumar, Tim K Marks, Wenxuan Mou, Ye Wang, Michael Jones, Anoop Cherian, Toshiaki Koike-Akino, Xiaoming Liu, and Chen Feng. Luvli face alignment: Estimating landmarks’ location, uncertainty, and visibility likelihood. In *Proceedings of the IEEE/CVF Conference on Computer Vision and Pattern Recognition*, pages 8236–8246, 2020. 1, 2, 7
- [36] Maksim Kuprashevich and Irina Tolstykh. Mivolo: Multi-input transformer for age and gender estimation. *arXiv preprint arXiv:2307.04616*, 2023. 2, 3, 6
- [37] Xing Lan, Qinghao Hu, Qiang Chen, Jian Xue, and Jian Cheng. Hih: Towards more accurate face alignment via heatmap in heatmap. *arXiv preprint arXiv:2104.03100*, 2021. 2, 3, 7
- [38] Cheng-Han Lee, Ziwei Liu, Lingyun Wu, and Ping Luo. Maskgan: Towards diverse and interactive facial image manipulation. In *IEEE Conference on Computer Vision and Pattern Recognition (CVPR)*, 2020. 5, 6, 16
- [39] Gil Levi and Tal Hassner. Age and gender classification using convolutional neural networks. In *Proceedings of the IEEE conference on computer vision and pattern recognition workshops*, pages 34–42, 2015. 2
- [40] Hangyu Li, Nannan Wang, Xinpeng Ding, Xi Yang, and Xinbo Gao. Adaptively learning facial expression representation via cf labels and distillation. *IEEE Transactions on Image Processing*, 30:2016–2028, 2021. 3, 6
- [41] Jinpeng Li, Haibo Jin, Shengcai Liao, Ling Shao, and Pheng-Ann Heng. Repformer: Refinement pyramid transformer for robust facial landmark detection. *arXiv preprint arXiv:2207.03917*, 2022. 2
- [42] Shan Li, Weihong Deng, and JunPing Du. Reliable crowdsourcing and deep locality-preserving learning for expression recognition in the wild. In *Proceedings of the IEEE conference on computer vision and pattern recognition*, pages 2852–2861, 2017. 5, 6, 17
- [43] Wanhua Li, Xiaoke Huang, Jiwen Lu, Jianjiang Feng, and Jie Zhou. Learning probabilistic ordinal embeddings for uncertainty-aware regression. In *Proceedings of the IEEE/CVF conference on computer vision and pattern recognition*, pages 13896–13905, 2021. 1, 2
- [44] Xiangtai Li, Haobo Yuan, Wei Li, Henghui Ding, Size Wu, Wenwei Zhang, Yining Li, Kai Chen, and Chen Change Loy. Omg-seg: Is one model good enough for all segmentation? *arXiv preprint arXiv:2401.10229*, 2024. 3
- [45] Yong Li, Jiabei Zeng, Shiguang Shan, and Xilin Chen. Occlusion aware facial expression recognition using cnn with attention mechanism. *IEEE Transactions on Image Processing*, 28(5):2439–2450, 2018. 6
- [46] Chunze Lin, Beier Zhu, Quan Wang, Renjie Liao, Chen Qian, Jiwen Lu, and Jie Zhou. Structure-coherent deep feature learning for robust face alignment. *IEEE Transactions on Image Processing*, 30:5313–5326, 2021. 1, 2
- [47] Jinpeng Lin, Hao Yang, Dong Chen, Ming Zeng, Fang Wen, and Lu Yuan. Face parsing with roi tanh-warping. In *Proceedings of the IEEE/CVF Conference on Computer Vision and Pattern Recognition*, pages 5654–5663, 2019. 3
- [48] Hai Liu, Shuai Fang, Zhaoli Zhang, Duantengchuan Li, Ke Lin, and Jiazhang Wang. Mfdnet: Collaborative poses perception and matrix fisher distribution for head pose estimation. *IEEE Transactions on Multimedia*, 24:2449–2460, 2021. 7
- [49] Ziwei Liu, Ping Luo, Xiaogang Wang, and Xiaoou Tang. Deep learning face attributes in the wild. In *Proceedings of the IEEE international conference on computer vision*, pages 3730–3738, 2015. 7
- [50] Ziwei Liu, Ping Luo, Xiaogang Wang, and Xiaoou Tang. Deep learning face attributes in the wild. In *Proceedings*

- of International Conference on Computer Vision (ICCV), 2015. 5, 16, 17
- [51] Ling Luo, Dingyu Xue, and Xinglong Feng. Ehanet: An effective hierarchical aggregation network for face parsing. *Applied Sciences*, 10(9):3135, 2020. 6
  - [52] Upal Mahbub, Sayantan Sarkar, and Rama Chellappa. Segment-based methods for facial attribute detection from partial faces. *IEEE Transactions on Affective Computing*, 11(4):601–613, 2018. 7
  - [53] Longbiao Mao, Yan Yan, Jing-Hao Xue, and Hanzi Wang. Deep multi-task multi-label cnn for effective facial attribute classification. *IEEE Transactions on Affective Computing*, 13(2):818–828, 2020. 7
  - [54] Chen Mi, Baoxi Yuan, Peng Ma, Yingxia Guo, Le Qi, Feng Wang, Wenbo Wu, and Lingling Wang. Visibility prediction based on landmark detection in foggy weather. In *2020 International Conference on Robots & Intelligent System (ICRIS)*, pages 134–137, 2020. 1, 2
  - [55] Paul Micaelli, Arash Vahdat, Hongxu Yin, Jan Kautz, and Pavlo Molchanov. Recurrence without recurrence: Stable video landmark detection with deep equilibrium models. In *Proceedings of the IEEE/CVF Conference on Computer Vision and Pattern Recognition*, pages 22814–22825, 2023. 2
  - [56] Zuheng Ming, Junshi Xia, Muhammad Muzzamil Luqman, Jean-Christophe Burie, and Kaixing Zhao. Dynamic multi-task learning for face recognition with facial expression. *arXiv preprint arXiv:1911.03281*, 2019. 3
  - [57] Takeru Miyato, Shin-ichi Maeda, Masanori Koyama, and Shin Ishii. Virtual adversarial training: a regularization method for supervised and semi-supervised learning. *IEEE transactions on pattern analysis and machine intelligence*, 41(8):1979–1993, 2018. 1, 2
  - [58] Ali Mollahosseini, Behzad Hasani, and Mohammad H Mahoor. Affectnet: A database for facial expression, valence, and arousal computing in the wild. *IEEE Transactions on Affective Computing*, 10(1):18–31, 2017. 5, 17
  - [59] Erik Murphy-Chutorian, Anup Doshi, and Mohan Manubhai Trivedi. Head pose estimation for driver assistance systems: A robust algorithm and experimental evaluation. In *2007 IEEE intelligent transportation systems conference*, pages 709–714. IEEE, 2007. 2
  - [60] Kartik Narayan, Harsh Agarwal, Kartik Thakral, Surbhi Mittal, Mayank Vatsa, and Richa Singh. Df-platter: Multi-face heterogeneous deepfake dataset. In *Proceedings of the IEEE/CVF Conference on Computer Vision and Pattern Recognition*, pages 9739–9748, 2023. 2
  - [61] Kartik Narayan, Nithin Gopalakrishnan Nair, Jennifer Xu, Rama Chellappa, and Vishal M Patel. Petalface: Parameter efficient transfer learning for low-resolution face recognition. *arXiv preprint arXiv:2412.07771*, 2024. 2
  - [62] Kartik Narayan, Vibashan VS, and Vishal M Patel. Seg-face: Face segmentation of long-tail classes. *arXiv preprint arXiv:2412.08647*, 2024. 2
  - [63] Zhenxing Niu, Mo Zhou, Le Wang, Xinbo Gao, and Gang Hua. Ordinal regression with multiple output cnn for age estimation. In *Proceedings of the IEEE conference on computer vision and pattern recognition*, pages 4920–4928, 2016. 6
  - [64] Mehdi Noroozi and Paolo Favaro. Unsupervised learning of visual representations by solving jigsaw puzzles. In *European conference on computer vision*, pages 69–84. Springer, 2016. 1, 2
  - [65] Jakub Paplham, Vojt Franc, et al. A call to reflect on evaluation practices for age estimation: Comparative analysis of the state-of-the-art and a unified benchmark. In *Proceedings of the IEEE/CVF Conference on Computer Vision and Pattern Recognition*, pages 1196–1205, 2024. 6
  - [66] Lixiong Qin, Mei Wang, Chao Deng, Ke Wang, Xi Chen, Jiani Hu, and Weihong Deng. Swinface: a multi-task transformer for face recognition, expression recognition, age estimation and attribute estimation. *IEEE Transactions on Circuits and Systems for Video Technology*, 2023. 2, 3, 6, 7
  - [67] Lixiong Qin, Mei Wang, Xuannan Liu, Yuhang Zhang, Wei Deng, Xiaoshuai Song, Weiran Xu, and Weihong Deng. Faceptor: A generalist model for face perception. In *European Conference on Computer Vision*, pages 240–260. Springer, 2025. 2, 3, 6, 7
  - [68] Alec Radford, Jong Wook Kim, Chris Hallacy, Aditya Ramesh, Gabriel Goh, Sandhini Agarwal, Girish Sastry, Amanda Askell, Pamela Mishkin, Jack Clark, et al. Learning transferable visual models from natural language supervision. In *International conference on machine learning*, pages 8748–8763. PMLR, 2021. 3, 8
  - [69] Aditya Ramesh, Mikhail Pavlov, Gabriel Goh, Scott Gray, Chelsea Voss, Alec Radford, Mark Chen, and Ilya Sutskever. Zero-shot text-to-image generation. In *International Conference on Machine Learning*, pages 8821–8831. PMLR, 2021. 3
  - [70] Rajeev Ranjan, Vishal M Patel, and Rama Chellappa. Hyperface: A deep multi-task learning framework for face detection, landmark localization, pose estimation, and gender recognition. *IEEE transactions on pattern analysis and machine intelligence*, 41(1):121–135, 2017. 3
  - [71] Rajeev Ranjan, Swami Sankaranarayanan, Carlos D Castillo, and Rama Chellappa. An all-in-one convolutional neural network for face analysis. In *2017 12th IEEE international conference on automatic face & gesture recognition (FG 2017)*, pages 17–24. IEEE, 2017. 3
  - [72] Karl Ricanek and Tamirat Tesafaye. Morph: A longitudinal image database of normal adult age-progression. In *7th international conference on automatic face and gesture recognition (FGR06)*, pages 341–345. IEEE, 2006. 17
  - [73] Ethan M Rudd, Manuel Günther, and Terrance E Boulton. Moon: A mixed objective optimization network for the recognition of facial attributes. In *Computer Vision—ECCV 2016: 14th European Conference, Amsterdam, The Netherlands, October 11–14, 2016, Proceedings, Part V 14*, pages 19–35. Springer, 2016. 7
  - [74] Nataniel Ruiz, Eunji Chong, and James M Rehg. Fine-grained head pose estimation without keypoints. In *Proceedings of the IEEE conference on computer vision and pattern recognition workshops*, pages 2074–2083, 2018. 7
  - [75] Christos Sagonas, Georgios Tzimiropoulos, Stefanos Zafeiriou, and Maja Pantic. 300 faces in-the-wild chal-

- lenge: The first facial landmark localization challenge. In *Proceedings of the IEEE international conference on computer vision workshops*, pages 397–403, 2013. 5, 16
- [76] Mausoom Sarkar, Mayur Hemani, Rishabh Jain, Balaji Krishnamurthy, et al. Parameter efficient local implicit image function network for face segmentation. In *Proceedings of the IEEE/CVF Conference on Computer Vision and Pattern Recognition*, pages 20970–20980, 2023. 3, 6
- [77] Jiahui She, Yibo Hu, Hailin Shi, Jun Wang, Qiu Shen, and Tao Mei. Dive into ambiguity: Latent distribution mining and pairwise uncertainty estimation for facial expression recognition. In *Proceedings of the IEEE/CVF conference on computer vision and pattern recognition*, pages 6248–6257, 2021. 3, 6
- [78] Jie Shen, Stefanos Zafeiriou, Grigoris G Chrysos, Jean Kossai, Georgios Tzimiropoulos, and Maja Pantic. The first facial landmark tracking in-the-wild challenge: Benchmark and results. In *Proceedings of the IEEE international conference on computer vision workshops*, pages 50–58, 2015. 5, 16
- [79] Nyeong-Ho Shin, Seon-Ho Lee, and Chang-Su Kim. Moving window regression: A novel approach to ordinal regression. In *Proceedings of the IEEE/CVF conference on computer vision and pattern recognition*, pages 18760–18769, 2022. 6
- [80] Ying Shu, Yan Yan, Si Chen, Jing-Hao Xue, Chunhua Shen, and Hanzi Wang. Learning spatial-semantic relationship for facial attribute recognition with limited labeled data. In *Proceedings of the IEEE/CVF Conference on Computer Vision and Pattern Recognition*, pages 11916–11925, 2021. 2, 3, 7
- [81] Dominykas Strazdas, Jan Hintz, and Ayoub Al-Hamadi. Robo-hud: Interaction concept for contactless operation of industrial cobotic systems. *Applied Sciences*, 11(12):5366, 2021. 2
- [82] Carole H Sudre, Wenqi Li, Tom Vercauteren, Sebastien Ourselin, and M Jorge Cardoso. Generalised dice overlap as a deep learning loss function for highly unbalanced segmentations. In *Deep Learning in Medical Image Analysis and Multimodal Learning for Clinical Decision Support: Third International Workshop, DLMIA 2017, and 7th International Workshop, ML-CDS 2017, Held in Conjunction with MICCAI 2017, Québec City, QC, Canada, September 14, Proceedings 3*, pages 240–248. Springer, 2017. 5
- [83] Haomiao Sun, Mingjie He, Shiguang Shan, Hu Han, and Xilin Chen. Task-adaptive q-face. *arXiv preprint arXiv:2405.09059*, 2024. 2, 3, 6, 7
- [84] Yi Sun, Yuheng Chen, Xiaogang Wang, and Xiaoou Tang. Deep learning face representation by joint identification-verification. *Advances in neural information processing systems*, 27, 2014. 1, 2
- [85] Yaniv Taigman, Ming Yang, Marc’Aurelio Ranzato, and Lior Wolf. Deepface: Closing the gap to human-level performance in face verification. In *Proceedings of the IEEE conference on computer vision and pattern recognition*, pages 1701–1708, 2014. 1, 2
- [86] Gusi Te, Yinglu Liu, Wei Hu, Hailin Shi, and Tao Mei. Edge-aware graph representation learning and reasoning for face parsing. In *Computer Vision–ECCV 2020: 16th European Conference, Glasgow, UK, August 23–28, 2020, Proceedings, Part XII 16*, pages 258–274. Springer, 2020. 2, 3, 6
- [87] Gusi Te, Wei Hu, Yinglu Liu, Hailin Shi, and Tao Mei. Agrnet: Adaptive graph representation learning and reasoning for face parsing. *IEEE Transactions on Image Processing*, 30:8236–8250, 2021. 3, 6
- [88] Hugo Touvron, Thibaut Lavril, Gautier Izacard, Xavier Martinet, Marie-Anne Lachaux, Timothée Lacroix, Baptiste Rozière, Naman Goyal, Eric Hambro, Faisal Azhar, et al. Llama: Open and efficient foundation language models. *arXiv preprint arXiv:2302.13971*, 2023. 3
- [89] Roberto Valle, José M Buenaposada, Antonio Valdés, and Luis Baumela. Face alignment using a 3d deeply-initialized ensemble of regression trees. *Computer Vision and Image Understanding*, 189:102846, 2019. 3, 6
- [90] Roberto Valle, José M Buenaposada, and Luis Baumela. Multi-task head pose estimation in-the-wild. *IEEE Transactions on Pattern Analysis and Machine Intelligence*, 43(8):2874–2881, 2020. 2, 3, 6, 7
- [91] Ashish Vaswani, Noam Shazeer, Niki Parmar, Jakob Uszkoreit, Llion Jones, Aidan N Gomez, Łukasz Kaiser, and Illia Polosukhin. Attention is all you need. *Advances in neural information processing systems*, 30, 2017. 3
- [92] Jingdong Wang, Ke Sun, Tianheng Cheng, Borui Jiang, Chaorui Deng, Yang Zhao, Dong Liu, Yadong Mu, Mingui Tan, Xinggang Wang, et al. Deep high-resolution representation learning for visual recognition. *IEEE transactions on pattern analysis and machine intelligence*, 43(10):3349–3364, 2020. 3, 7
- [93] Junke Wang, Dongdong Chen, Zuxuan Wu, Chong Luo, Luowei Zhou, Yucheng Zhao, Yujia Xie, Ce Liu, Yu-Gang Jiang, and Lu Yuan. Omnivl: One foundation model for image-language and video-language tasks. *Advances in neural information processing systems*, 35:5696–5710, 2022. 3
- [94] Kai Wang, Xiaojiang Peng, Jianfei Yang, Shijian Lu, and Yu Qiao. Suppressing uncertainties for large-scale facial expression recognition. In *Proceedings of the IEEE/CVF conference on computer vision and pattern recognition*, pages 6897–6906, 2020. 6
- [95] Kai Wang, Xiaojiang Peng, Jianfei Yang, Debin Meng, and Yu Qiao. Region attention networks for pose and occlusion robust facial expression recognition. *IEEE Transactions on Image Processing*, 29:4057–4069, 2020. 6
- [96] Qianqian Wang, Yen-Yu Chang, Ruojin Cai, Zhengqi Li, Bharath Hariharan, Aleksander Holynski, and Noah Snavely. Tracking everything everywhere all at once. *arXiv preprint arXiv:2306.05422*, 2023. 3
- [97] Zhenyu Wang, Yali Li, Xi Chen, Ser-Nam Lim, Antonio Torralba, Hengshuang Zhao, and Shengjin Wang. Detecting everything in the open world: Towards universal object detection. In *Proceedings of the IEEE/CVF Conference on Computer Vision and Pattern Recognition*, pages 11433–11443, 2023. 3
- [98] Zhen Wei, Yao Sun, Jinqiao Wang, Hanjiang Lai, and Si Liu. Learning adaptive receptive fields for deep image pars-



- ing network. In *Proceedings of the IEEE conference on computer vision and pattern recognition*, pages 2434–2442, 2017. 1, 2
- [99] Zhen Wei, Si Liu, Yao Sun, and Hefei Ling. Accurate facial image parsing at real-time speed. *IEEE Transactions on Image Processing*, 28(9):4659–4670, 2019. 6
- [100] Tiancheng Wen, Zhonggan Ding, Yongqiang Yao, Yaxiong Wang, and Xueming Qian. Picassonet: Searching adaptive architecture for efficient facial landmark localization. *IEEE Transactions on Neural Networks and Learning Systems*, 34(12):10516–10527, 2023. 7
- [101] Lior Wolf, Tal Hassner, and Yaniv Taigman. Effective unconstrained face recognition by combining multiple descriptors and learned background statistics. *IEEE transactions on pattern analysis and machine intelligence*, 33(10):1978–1990, 2010. 5, 17
- [102] Erroll Wood, Tadas Baltrušaitis, Charlie Hewitt, Matthew Johnson, Jingjing Shen, Nikola Milosavljević, Daniel Wilde, Stephan Garbin, Toby Sharp, Ivan Stojiljković, et al. 3d face reconstruction with dense landmarks. In *European Conference on Computer Vision*, pages 160–177. Springer, 2022. 1, 2
- [103] Wayne Wu, Chen Qian, Shuo Yang, Quan Wang, Yici Cai, and Qiang Zhou. Look at boundary: A boundary-aware face alignment algorithm. In *Proceedings of the IEEE conference on computer vision and pattern recognition*, pages 2129–2138, 2018. 7
- [104] Yue Wu and Qiang Ji. Robust facial landmark detection under significant head poses and occlusion. In *Proceedings of the IEEE International Conference on Computer Vision*, pages 3658–3666, 2015. 6
- [105] Yue Wu, Chao Gou, and Qiang Ji. Simultaneous facial landmark detection, pose and deformation estimation under facial occlusion. In *Proceedings of the IEEE conference on computer vision and pattern recognition*, pages 3471–3480, 2017. 6
- [106] Jiahao Xia, Weiwei Qu, Wenjian Huang, Jianguo Zhang, Xi Wang, and Min Xu. Sparse local patch transformer for robust face alignment and landmarks inherent relation learning. In *Proceedings of the IEEE/CVF Conference on Computer Vision and Pattern Recognition*, pages 4052–4061, 2022. 3, 7
- [107] Enze Xie, Wenhai Wang, Zhiding Yu, Anima Anandkumar, Jose M Alvarez, and Ping Luo. Segformer: Simple and efficient design for semantic segmentation with transformers. *Advances in Neural Information Processing Systems*, 34:12077–12090, 2021. 4
- [108] Miao Xin, Shentong Mo, and Yuanze Lin. Eva-gcn: Head pose estimation based on graph convolutional networks. In *Proceedings of the IEEE/CVF Conference on computer vision and pattern recognition*, pages 1462–1471, 2021. 7
- [109] Xinchen Yan, Jimei Yang, Kihyuk Sohn, and Honglak Lee. Attribute2image: Conditional image generation from visual attributes. In *Computer Vision–ECCV 2016: 14th European Conference, Amsterdam, The Netherlands, October 11–14, 2016, Proceedings, Part IV 14*, pages 776–791. Springer, 2016. 1, 2
- [110] Tsun-Yi Yang, Yi-Ting Chen, Yen-Yu Lin, and Yung-Yu Chuang. Fsa-net: Learning fine-grained structure aggregation for head pose estimation from a single image. In *Proceedings of the IEEE/CVF conference on computer vision and pattern recognition*, pages 1087–1096, 2019. 7
- [111] Xiangnan Yin, Di Huang, Zehua Fu, Yunhong Wang, and Liming Chen. Segmentation-reconstruction-guided facial image de-occlusion. In *2023 IEEE 17th International Conference on Automatic Face and Gesture Recognition (FG)*, pages 1–8. IEEE, 2023. 1, 2
- [112] Lu Yuan, Dongdong Chen, Yi-Ling Chen, Noel Codella, Xiyang Dai, Jianfeng Gao, Houdong Hu, Xuedong Huang, Boxin Li, Chunyuan Li, et al. Florence: A new foundation model for computer vision. *arXiv preprint arXiv:2111.11432*, 2021. 3
- [113] Alireza Zaeemzadeh, Shabnam Ghadar, Baldo Faieta, Zhe Lin, Nazanin Rahnavard, Mubarak Shah, and Ratheesh Kalarot. Face image retrieval with attribute manipulation. In *Proceedings of the IEEE/CVF International Conference on Computer Vision*, pages 12116–12125, 2021. 1, 2
- [114] Jiabei Zeng, Shiguang Shan, and Xilin Chen. Facial expression recognition with inconsistently annotated datasets. In *Proceedings of the European conference on computer vision (ECCV)*, pages 222–237, 2018. 6
- [115] Cheng Zhang, Hai Liu, Yongjian Deng, Bochen Xie, and Youfu Li. Tokenhpe: Learning orientation tokens for efficient head pose estimation via transformers. In *Proceedings of the IEEE/CVF Conference on Computer Vision and Pattern Recognition*, pages 8897–8906, 2023. 2, 3, 5, 7
- [116] Hongwen Zhang, Qi Li, Zhenan Sun, and Yunfan Liu. Combining data-driven and model-driven methods for robust facial landmark detection. *IEEE Transactions on Information Forensics and Security*, 13(10):2409–2422, 2018. 6
- [117] Hao Zhang, Mengmeng Wang, Yong Liu, and Yi Yuan. Fdn: Feature decoupling network for head pose estimation. In *Proceedings of the AAAI conference on artificial intelligence*, pages 12789–12796, 2020. 3
- [118] Ning Zhang, Manohar Paluri, Marc’Aurelio Ranzato, Trevor Darrell, and Lubomir Bourdev. Panda: Pose aligned networks for deep attribute modeling. In *Proceedings of the IEEE conference on computer vision and pattern recognition*, pages 1637–1644, 2014. 7, 15
- [119] Zhanpeng Zhang, Ping Luo, Chen Change Loy, and Xiaoou Tang. Facial landmark detection by deep multi-task learning. In *Computer Vision–ECCV 2014: 13th European Conference, Zurich, Switzerland, September 6–12, 2014, Proceedings, Part VI 13*, pages 94–108. Springer, 2014. 3
- [120] Zhifei Zhang, Yang Song, and Hairong Qi. Age progression/regression by conditional adversarial autoencoder. In *Proceedings of the IEEE conference on computer vision and pattern recognition*, pages 5810–5818, 2017. 5, 17
- [121] Rui Zhao, Tianshan Liu, Jun Xiao, Daniel PK Lun, and Kin-Man Lam. Deep multi-task learning for facial expression recognition and synthesis based on selective feature sharing. In *2020 25th International Conference on Pattern Recognition (ICPR)*, pages 4412–4419. IEEE, 2021. 3
- [122] Qingping Zheng, Jiankang Deng, Zheng Zhu, Ying Li, and Stefanos Zafeiriou. Decoupled multi-task learning with

- cyclical self-regulation for face parsing. In *Proceedings of the IEEE/CVF conference on computer vision and pattern recognition*, pages 4156–4165, 2022. 2, 3, 6
- [123] Yinglin Zheng, Hao Yang, Ting Zhang, Jianmin Bao, Dongdong Chen, Yangyu Huang, Lu Yuan, Dong Chen, Ming Zeng, and Fang Wen. General facial representation learning in a visual-linguistic manner. In *Proceedings of the IEEE/CVF Conference on Computer Vision and Pattern Recognition*, pages 18697–18709, 2022. 2, 3, 6, 7
- [124] Yijun Zhou and James Gregson. Whenet: Real-time fine-grained estimation for wide range head pose. *arXiv preprint arXiv:2005.10353*, 2020. 1, 2, 3, 7
- [125] Zhenglin Zhou, Huaxia Li, Hong Liu, Nanyang Wang, Gang Yu, and Rongrong Ji. Star loss: Reducing semantic ambiguity in facial landmark detection. In *Proceedings of the IEEE/CVF Conference on Computer Vision and Pattern Recognition*, pages 15475–15484, 2023. 1, 2, 3, 5, 15
- [126] Jiawen Zhu, Simiao Lai, Xin Chen, Dong Wang, and Huchuan Lu. Visual prompt multi-modal tracking. In *Proceedings of the IEEE/CVF Conference on Computer Vision and Pattern Recognition*, pages 9516–9526, 2023. 3
- [127] Peihao Zhu, Rameen Abdal, Yipeng Qin, and Peter Wonka. Sean: Image synthesis with semantic region-adaptive normalization. In *Proceedings of the IEEE/CVF Conference on Computer Vision and Pattern Recognition*, pages 5104–5113, 2020. 1, 2
- [128] Xiangyu Zhu, Zhen Lei, Xiaoming Liu, Hailin Shi, and Stan Z Li. Face alignment across large poses: A 3d solution. In *Proceedings of the IEEE conference on computer vision and pattern recognition*, pages 146–155, 2016. 5, 16
- [129] Xizhou Zhu, Weijie Su, Lewei Lu, Bin Li, Xiaogang Wang, and Jifeng Dai. Deformable detr: Deformable transformers for end-to-end object detection. *arXiv preprint arXiv:2010.04159*, 2020. 4
- [130] Zheng Zhu, Guan Huang, Jiankang Deng, Yun Ye, Junjie Huang, Xinze Chen, Jiagang Zhu, Tian Yang, Jiwen Lu, Dalong Du, et al. Webface260m: A benchmark unveiling the power of million-scale deep face recognition. In *Proceedings of the IEEE/CVF Conference on Computer Vision and Pattern Recognition*, pages 10492–10502, 2021. 8
- [131] Ni Zhuang, Yan Yan, Si Chen, and Hanzi Wang. Multi-task learning of cascaded cnn for facial attribute classification. In *2018 24th International Conference on Pattern Recognition (ICPR)*, pages 2069–2074. IEEE, 2018. 3, 7
- [132] Xueyan Zou, Jianwei Yang, Hao Zhang, Feng Li, Linjie Li, Jianfeng Wang, Lijuan Wang, Jianfeng Gao, and Yong Jae Lee. Segment everything everywhere all at once. *Advances in Neural Information Processing Systems*, 36, 2024. 3

# Appendix

## A. Overview

As part of the Appendix, we present the following as an extension to the ones shown in the paper:

- Cross-dataset Evaluation (Section B)
- Ablation study (Section C)
- In-the-wild Visualization (Section D)
- Dataset details (Section E)

## B. Cross-Dataset Evaluation

We conduct additional cross-dataset experiments to demonstrate the effectiveness of *FaceXFormer* in scenarios that closely resemble real-life conditions. These scenarios involve previously unseen, unconstrained face images characterized by significant variability in background, lighting, pose, and other factors. As shown in Table B.1, *FaceXFormer* outperforms the existing state-of-the-art model, STARLoss [125], on the 300VW dataset. This highlights *FaceXFormer*'s effectiveness in landmark detection under in-the-wild scenarios. The cross-dataset results support the rationale presented in this paper: the necessity of a unified facial analysis model capable of performing multiple tasks on unconstrained, in-the-wild faces, particularly for real-time applications. *FaceXFormer* addresses this gap and achieves state-of-the-art performance.

| Method                    | 300VW (Cat.A) | 300VW (Cat.B) | 300VW (Cat.C) | LFWA (Gender) |
|---------------------------|---------------|---------------|---------------|---------------|
|                           | NME           | NME           | NME           | Acc.          |
| PANDA [118]               | -             | -             | -             | 92.00         |
| STARLoss [125]            | 3.97          | <b>3.39</b>   | 8.42          | -             |
| <b><i>FaceXFormer</i></b> | <b>3.90</b>   | 3.58          | <b>6.75</b>   | <b>92.74</b>  |

Table B.1. Cross Dataset evaluation of *FaceXFormer*.

## C. Ablation Study

To evaluate the contribution of each component in *FaceXFormer*, we conduct an ablation study focusing on the importance of specific design choices and their impact on performance across various tasks. Specifically, we perform experiments by: a) Excluding multi-scale features and relying solely on the final-layer features. b) Removing the FXDec decoder from the architecture. The results of these experiments are summarized in Table C.1.

| Method                    | HPE         | Lnd         | Attr.        | Age         |
|---------------------------|-------------|-------------|--------------|-------------|
|                           | F1          | MAE         | Acc.         | MAE         |
| w/o multi-scale           | 3.70        | 4.70        | 91.21        | 4.21        |
| w/o FXDec                 | 17.16       | 31.49       | 79.90        | 16.15       |
| <b><i>FaceXFormer</i></b> | <b>3.52</b> | <b>4.67</b> | <b>91.83</b> | <b>4.17</b> |

Table C.1. Impact of various components of *FaceXFormer* on performance.

From the results, it is evident that the FXDec decoder, which incorporates self-attention and interactions between face tokens and task tokens, plays a critical role in performance. Without FXDec, there is a significant drop across all tasks. For instance, the Mean Absolute Error (MAE) for landmark detection increases from 4.67 to 31.49, and the accuracy for attribute classification drops from 91.83% to 79.90%. This substantial decline highlights the decoder's importance in effectively capturing complex feature relationships necessary for these tasks. Similarly, excluding multi-scale features leads to reduced performance across all tasks, with a particularly notable impact on head pose estimation and age estimation. The F1 score for head pose estimation increases from 3.52 to 3.70 (indicating worse performance since lower is better), and the MAE for





twice). The head pose range spans approximately  $\pm 75^\circ$  yaw and  $\pm 60^\circ$  pitch. During training, we loosely crop the face images based on the landmarks and apply several augmentations, including random gray (10%), random Gaussian blur (10%), random resized crop (80% to 100%) and random gamma adjustment (10%).

#### E.4. Attributes Prediction

We utilize the CelebA [50] dataset for training and the LFWA [101] dataset for cross-dataset evaluation of multi-task methods. CelebA comprises 202,599 facial images, each annotated with 40 binary labels that indicate various facial attributes such as hair color, attractive, bangs, big lips, and more. LFWA consists of 13,143 facial images, annotated with the same set of facial attributes. During training, we apply several augmentations, including random rotation ( $\pm 18^\circ$ ), random scaling ( $\pm 10\%$ ), random translation ( $1\% \times 224$ ), random horizontal flip (50%), random gray (10%), random Gaussian blur (10%), and random gamma adjustment (20%).

#### E.5. Age/Gender/Race Estimation

We utilize the FairFace [32] and UTKFace [120] datasets for training, and the FFHQ [33] dataset for cross-dataset testing. FairFace comprises 108,501 images, balanced across seven racial groups: White, Black, Indian, East Asian, Southeast Asian, Middle Eastern, and Latino. The UTKFace dataset contains 20,000 facial images annotated with age, gender, and race. In our work, we follow the 'race-4' annotation scheme, categorizing individuals into five racial labels: White, Black, Indian, Asian, and Others. Age annotations are categorized into decade bins: 0–9, 10–19, 20–29, 30–39, 40–49, 50–59, 60–69, and over 70. Gender is annotated with two labels: male and female. Additionally, we incorporate the MORPH-II dataset [72], which contains 55,134 facial images of 13,617 subjects aged between 16 and 77 years. This dataset provides annotations for age, gender, and race, with a predominance of male subjects and a significant representation of Black and White individuals. For age estimation tasks, we train on both UTKFace and MORPH-II datasets and evaluate our models on the MORPH-II dataset to assess performance. During training, we apply augmentations such as random rotation ( $\pm 18^\circ$ ), random scaling ( $\pm 10\%$ ), random translation ( $1\% \times 224$ ), random horizontal flip (50%), random grayscale conversion (10%), random Gaussian blur (10%), and random gamma adjustment (10%).

#### E.6. Facial Expression Recognition

We utilize the RAF-DB [42] and AffectNet [58] datasets for training and RAF-DB [42] dataset for intra-dataset evaluation. RAF-DB is a facial expression dataset with approximately 30,000 images. The dataset includes variability in subjects' age, gender, ethnicity, head poses, lighting conditions, and occlusions (e.g., glasses, facial hair, or self-occlusion). RAF-DB provides annotations for seven basic emotions that are surprise, fear, disgust, happiness, sadness, anger, and neutral. AffectNet is one of the largest facial expression datasets with approximately 440,000 images that are manually annotated for the presence of eight discrete facial expressions: neutral, happy, angry, sad, fear, surprise, disgust, contempt. During training, we apply augmentations such as random rotation ( $\pm 18^\circ$ ), random scaling ( $\pm 10\%$ ), random translation ( $1\% \times 224$ ), random horizontal flip (50%), random grayscale conversion (10%), random Gaussian blur (10%), random color jitter (10%), and random gamma adjustment (10%).

#### E.7. Visibility Prediction

We utilize the COFW [7] dataset, which is annotated with 29 landmarks for landmarks visibility prediction. Each landmark is associated with 29 binary labels that indicate its visibility. We loosely crop the faces and apply augmentations, including random horizontal flip (50%), random gray (10%), random Gaussian blur (10%), and random gamma adjustment (10%).